Diffraction-limited astronomical X-ray imaging and X-ray interferometry using normal-incidence multilayer optics

David L. Windt[*], Steven M. Kahn
Columbia Astrophysics Laboratory, 550 West 120th Street, New York, NY 10027

Gary E. Sommargren
Lawrence Livermore National Laboratory, 7000 East Avenue, Livermore, CA 94550

ABSTRACT

We describe a new technical approach for observations of Galactic and extra-Galactic soft X-ray sources with ultra-high angular resolution. The technique is based on the use of recently developed diffraction-limited, normal-incidence mirror substrates and ultra-short-period multilayer coatings, tuned to specific bright emission lines in the range $16 < \lambda < 40$ Å, for the construction of a diffraction-limited X-ray telescope. Sub-milliarcsecond resolution could be achieved in a moderately-sized Cassegrain or prime-focus geometry, while resolution of order 0.01 μas could be achieved using a synthetic aperture X-ray interferometer constructed from an array of such telescopes spread over a 50 km baseline. We describe our technical approach in detail and outline some of the observations that would become possible with the proposed instrumentation.

1. INTRODUCTION

Because the reflectance near normal incidence of even the best optical materials is exceedingly small in the X-ray band, the traditional approach towards the construction of astronomical X-ray telescopes uses mirrors that operate at grazing incidence, below the so-called 'critical angle' for total external reflection, where the X-ray reflectance is high. This approach has been refined over the past four decades of X-ray astronomy and solar physics, and the state-of-the-art (with regard to angular resolution) is embodied in the recently launched *Chandra* observatory, which achieves a point-spread-function of ~0.5 arcseconds FWHM. Although this resolution is clearly a remarkable achievement, it is nevertheless ~100X larger than the diffraction limit determined by the (annular) primary mirror aperture (i.e., outer diameter D=1.2 m.) The angular resolution in the case of such grazing incidence telescopes is limited primarily by surface figure errors in the mirrors, as these highly aspheric cylindrical (e.g., Wolter) surfaces are exceedingly difficult to fabricate and measure.

The limitations and difficulties associated with the construction of grazing incidence X-ray telescopes can be circumvented (albeit with some important limitations) by using normal-incidence X-ray mirrors employing multilayer coatings. Multilayer mirrors afford the ability to construct X-ray optical systems more akin to those used in the visible part of the spectrum, having low aberrations over a wide field of view, and comprising more conventional mirror substrates having greater finish and figure specifications. They offer some important performance advantages as well, discussed below. The multilayer coatings, developed largely over the past two decades, are designed to achieve constructive interference between reflections from each interface in the film, and thus provide high reflectance over a relatively narrow band of soft X-ray or EUV wavelengths, precisely tunable by adjusting the thickness of the individual layers that comprise the multilayer stack. Normal-incidence X-ray mirrors utilizing such coatings are now used in a variety of scientific disciplines, and in solar physics particularly. Solar EUV telescopes using multilayers tuned to specific coronal emission lines or line complexes have been used in a number of sounding rocket and satellite experiments, most notably the *SoHO EIT*[1] and *TRACE*[2,3] missions, and will be used in future missions as well, including *Solar-B, STEREO,* and the *Solar Dynamics Observatory*. Just as narrow-band filters are used routinely for high-

---

[*] windt@astro.columbia.edu

441

resolution 'monochromatic' imaging in the UV, visible and IR, the intrinsic narrow-band response of the multilayers in the soft X-ray and EUV is advantageous, and is in fact exploited to provide high-resolution 'monochromatic' coronal images; in some cases, the response of the coating is sufficiently narrow that images representing emission from single ion species are obtained. Wide spectral coverage (thus far in the range ~$60 < \lambda < 500$ Å) is achieved by using several discrete multilayer imaging channels. The high-resolution multilayer imaging data can be used to complement high-resolution spectral data and thus provide a unique observational probe directed at understanding the physics of the solar corona, i.e., thermal structure, energy transfer, magnetic fields and surface flows, solar active regions, coronal mass ejections, etc.

As a result of recent technological achievements, in particular the availability of both large-diameter, diffraction-limited X-ray mirror substrates and ultra-short-period multilayers that operate at wavelengths as short as ~16 Å at normal incidence, the approach now widely used in the EUV for solar physics just described can be extended to the shorter soft X-ray wavelengths appropriate for observations of both Galactic and extra-Galactic X-ray sources (i.e., where absorption by the interstellar medium is minimal.) In the wavelength range $16 < \lambda < 40$ Å in particular, which includes a number of bright emission lines observed in a variety of astronomical sources, using currently-available multilayer X-ray mirror technology, sub-milliarcsecond resolution and narrow-band effective area in the range ~1 – 65 cm^2 (depending on the wavelength) could be achieved with a moderately-sized Cassegrain-type telescope geometry, i.e., ~2.5 m diameter x 10 m focal length, and even greater effective area – in the range of 75 – 2500 cm^2 – with a 2.5-m-diameter prime-focus geometry; further in the future, we can hope to achieve resolution of order 0.01 µas or greater and effective area in the range 0.2 – 8 m^2 (or more) using an X-ray interferometer (as for the currently-envisioned *MAXIM* mission[4]) constructed from an array of prime-focus multilayer telescopes spread, for example, over a 50 km baseline. Space observatories based on this technology would enable a wide range of fundamentally new astronomical investigations.

The purpose of this article is to increase community awareness of the current capabilities of normal incidence multilayer X-ray optics, in order to facilitate and encourage wider participation in continued research and development that will allow us to realize the full potential of this technology with regard to space astronomy. In §2 we describe the multilayer mirror technology on which our instrumental approach is based. We outline some specific instrument concepts in §3 in more detail, and describe some of the astronomical observations that would become possible with this instrumentation in §4. We conclude in §5 with a brief summary and discussion of future prospects.

2. NORMAL INCIDENCE X-RAY MULTILAYER MIRRORS

The technical feasibility of the instrument concepts outlined in §3 are based on recently developed X-ray optical technology comprising diffraction-limited mirror substrates and ultra-short-period X-ray multilayer coatings. We discuss the current state-of-the-art of these two technologies in §2.1 and §2.2 below.

2.1 DIFFRACTION-LIMITED MIRROR SUBSTRATES

It is perhaps not widely recognized among the astronomical X-ray optics community that diffraction-limited X-ray mirrors have already been developed, and are, in fact, now in regular use. For more than a decade, a concerted worldwide effort driven by the international semiconductor industry has been directed at the development of diffraction-limited EUV imaging systems for photo-lithography, an approach now known as Extreme Ultraviolet Lithography (EUVL). The EUVL imaging systems utilize multilayer mirrors with coatings tuned to $\lambda\sim134$ Å, where the reflectance of normal-incidence Mo/Si multilayers has approached 70%. The multilayers are deposited onto aspherical mirror substrates (having ~1 µm spherical departure) as large as 20 – 25 cm in diameter. The spatial resolution of a diffraction-limited imaging system is proportional to λ/NA, where NA is the system numerical aperture; at present, multiple-reflection EUVL imaging systems using large-diameter multilayer mirrors achieve diffraction-limited spatial resolution of less than 0.10 µm over a ~2.5 cm field,[5] with even greater resolution goals for the future. The spatial resolution currently achievable corresponds to an angular resolution of ~26 milliarcseconds (i.e., at λ=134 Å), over a field of 1.79° (assuming an effective focal length of 0.8 m.)

As a result of the EUVL effort, large-diameter mirror substrates having 1–2 Å figure and finish specifications are now commercially available, as are new metrology tools needed to characterize these substrates and facilitate their fabrication, such as the LLNL point-diffraction interferometer operating in the visible,[6] as well as synchrotron-based 'at-

wavelength' interferometers,[7] both having sub-nm precision. The EUVL substrates are diffraction-limited to $\sim\lambda_{134\text{Å}}/50$, and at the shorter soft X-ray wavelengths of interest for astronomy, to $\sim\lambda_{34\text{Å}}/10$, or $\sim\lambda_{17\text{Å}}/5$, sufficient to construct a two-reflection diffraction-limited astronomical telescope.

2.1 ULTRA-SHORT-PERIOD X-RAY MULTILAYERS

In the past two years new multilayer coatings have become available that are designed for normal-incidence reflection in the soft X-ray band appropriate for non-solar astronomical observations. In particular, two systems, Cr/Sc and W/B$_4$C, now can be used as normal incidence mirror coatings in the range λ=16 – 40 Å. These coatings can be deposited onto large-diameter figured mirror substrates, using multilayer deposition systems developed just over the past decade that are capable of sub-angstrom control of the coating thickness uniformity, as is necessary to ensure both maximal system throughput, and minimal coating-induced wavefront distortions.[8,9]

Cr/Sc multilayers work best in the range 31 – 40 Å, above the Sc L-edge where absorption in the Sc layers is minimal.[10,11] The measured normal-incidence reflectance of three typical Cr/Sc multilayers are shown in Fig. 1a; these films each contain 300 bilayers, with periods in the range $d\sim$16–19 Å. Interpolating from the data in Fig. 1a, we infer a peak reflectance at normal incidence (θ=2.5°) of R=5% at λ=33.7 Å, i.e., corresponding to the wavelength of the C VI Ly-α emission line observed in many astrophysical plasmas. (The films shown in Fig. 1a are illustrative examples. An actual astronomical telescope would use a Cr/Sc multilayer coating tuned precisely to the C VI line.) The multilayer bandwidth is $\Delta\lambda$=0.12 Å FWHM (i.e., $\lambda/\Delta\lambda\sim$300), and is well-matched to the width of the C VI line in many cases.

At shorter wavelengths, W/B$_4$C multilayers having periods as small as d=8 Å can be used as normal incidence reflective coatings at wavelengths as short as $\lambda\sim$16 Å.[12] Although the absorption in the W and B$_4$C layers is not as low as in other candidate materials having K- or L-edges in this spectral range, it has recently been shown that by properly adjusting the fractional W-layer-thickness, W/B$_4$C multilayers can be grown with interface widths as small as σ=2.9 Å, so that the attainable reflectance at normal incidence is higher than with other available multilayer systems thus far investigated. Example

(a)

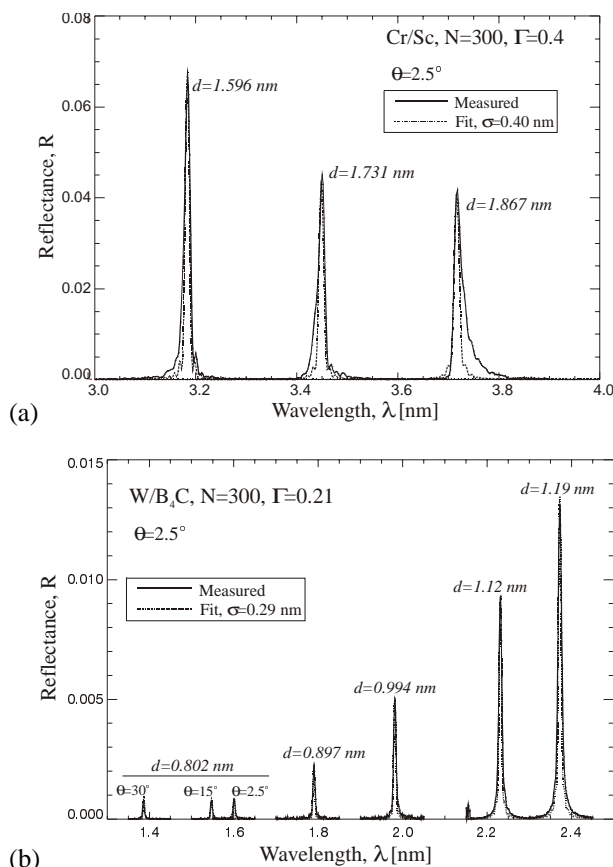

(b)

Figure 1. Normal-incidence reflectance, measured as a function of wavelength using synchrotron radiation, of periodic Cr/Sc (a) and W/B$_4$C (b) multilayers, containing N=300 bilayers, and having the multilayer periods d as indicated.
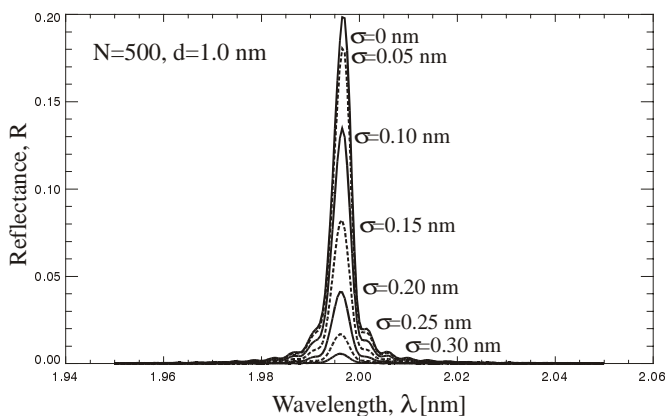

Figure 2. Theoretical reflectance of periodic W/B$_4$C multilayers containing 500 bilayers, with d=1.0 nm, and interface widths in the range σ=0 – 0.3 nm as indicated.

reflectance curves for five W/B_4C multilayers, all containing 300 bilayers, with periods in the range $8 < d < 12$ Å are shown in Fig. 1b. The normal incidence ($\theta=2.5°$) peak reflectance for structures containing N=300 periods was measured to range from 1.3% at $\lambda=24$ Å ($d=12$ Å) to 0.08% at $\lambda=16$ Å ($d=8$ Å); the bandwidths were found to range from $\Delta\lambda\sim0.08$ Å ($d=12$ Å) to $\Delta\lambda\sim0.06$ Å ($d=8$ Å), and agree well with the theoretical values, indicating good stability of the deposition rates during growth. The spectral region over which these multilayers operate includes the bright emission lines of N VII ($\lambda=24.8$ Å), O VII ($\lambda=22.1$ Å), O VIII ($\lambda=19.0$ Å), and Fe XVII ($\lambda=17.0$ Å), all observed in many astrophysical plasmas.

As will be discussed in §3 below, the currently available performance of these Cr/Sc and W/B_4C multilayer coatings is sufficient to construct astronomical telescopes having sensitivity high enough for a range of new observations. Nevertheless, ongoing multilayer research will almost certainly lead to even greater performance in the future. For instance, in the case of the W/B_4C films shown in Fig. 1b, simply increasing the number of bilayers from N=300 to N=600 is expected to increase the peak reflectance by a factor of $\sim1.5 - 2.1$ (depending on the wavelength). Furthermore, even small improvements in the interface morphology in these structures will lead to significant performance gains as well. To illustrate, shown in Fig. 2 are theoretical reflectance curves for W/B_4C multilayers having $d=10$ Å, N=500, and interface widths in the range $\sigma=0 - 3$ Å; by further optimizing the multilayer deposition process so that the interface widths are reduced from $\sigma=2.9$ Å to $\sigma=1.5$ Å, an additional factor of ~10 in peak normal-incidence reflectance plausibly could be realized.   Finally, it might be possible eventually to develop other multilayer systems, comprising materials having larger optical contrast and/or more perfect interfaces, and thus having even better soft X-ray performance.

3. INSTRUMENT CONCEPTS

Given the existing technological infrastructure now available for the production and metrology of the requisite mirror substrates, and for the deposition of ultra-short-period multilayers onto such substrates (with the necessary coating uniformity control), as just described, we can envision a variety of new astronomical instruments, ranging from Cassegrain-type and prime-focus telescopes, to a multiple-mirror X-ray interferometer. We outline these instrument concepts in the subsections that follow.

3.1 A MONOCHROMATIC CASSEGRAIN-TYPE TELESCOPE

A diffraction-limited Cassegrain-type telescope constructed from normal-incidence multilayer X-ray optics is shown schematically in Fig. 3. In this example system, we have selected a 2.5-m-diameter primary mirror having a radius of curvature R=20 m, and an 11-mm-diameter secondary mirror having R=68 mm, so th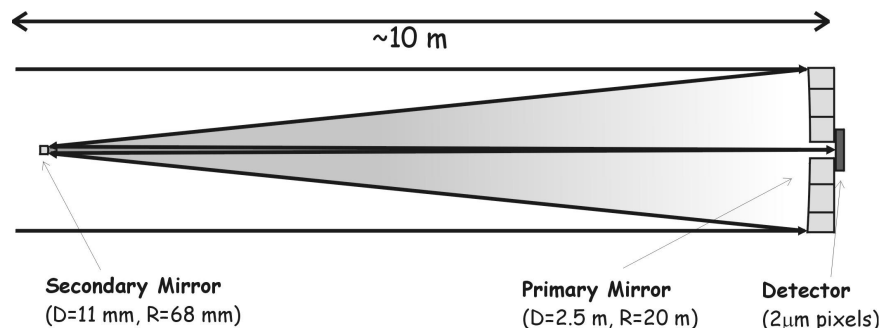at the effective focal length of the system is 10 m, and one resolution element fills an area of 4 μm in the focal plane.

Figure 3. Conceptual diagram of an X-ray multilayer Cassegrain-type telescope having sub-mas angular resolution.

An imaging detector having 2 μm pixels thus would be needed in order to provide two pixels per resolution element.

As summarized in Table 1, the diffraction-limited resolution of this system ranges from $\delta\theta=\lambda/D=0.28$ mas to $\delta\theta=0.14$ mas over the wavelength range $\lambda=33.7$ to 17 Å. The system would be designed for monochromatic imaging at a pre-selected wavelength, corresponding to one of the ions (i.e., C VI through Fe XVII) listed in the table, and the multilayer coatings thus would be tuned appropriately. After the two multilayer reflections, the effective area of this instrument ranges from $A_{eff}=123$ cm^2 at the C VI line to $A_{eff}=0.1$ cm^2 at Fe XVII. (The addition of a 1500-Å-thick Al filter, needed to suppress visible light, would result in an additional efficiency loss of 0.48 ($\lambda=33.7$Å) to 0.11 ($\lambda=17$ Å) in this instrument.)

To construct the telescope optics, the primary mirror would likely be segmented, with individual mirror segments limited in size to ~25 cm, so that currently available fabrication, metrology and coating facilities could be utilized. Although many additionally engineering challenges remain to be addressed in order construct such an instrument, particularly with regard to alignment, stability, and pointing, the overall size of the instrument is such that it could fit in a single spacecraft.

3.2 A MONOCHROMATIC PRIME-FOCUS TELESCOPE

An even more ambitious instrument as compared to the Cassegrain system of Fig. 3, comprising a prime-focus multilayer telescope mirror (R_c=20 km) and a detector (5 μm pixels) located on a separate spacecraft 10 km away, is shown in Fig. 4. (The mirror-detector separation, and the mirror radius of
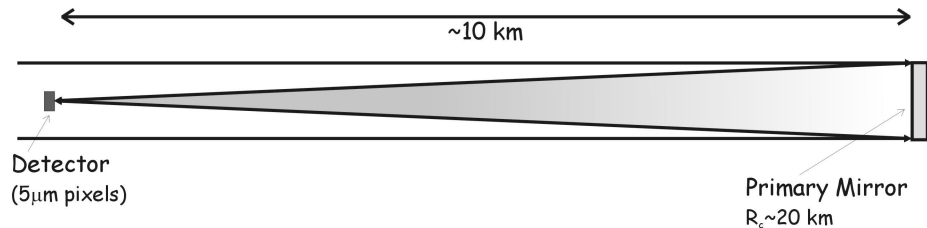

Figure 4. Conceptual diagram of an X-ray multilayer prime-focus telescope having sub-mas angular resolution.

curvature scale linearly with the detector pixel size; these parameters thus can be adjusted as desired, in accord with the appropriate engineering constraints.) Assuming again a 2.5-m primary mirror, the angular resolution of this system is identical to that of the Cassegrain. In this case, however, because there is only a single multilayer reflection, the effective area is much greater, ranging from A_{eff}=2,454 cm^2 at the C VI line to A_{eff}=74 cm^2 at Fe XVII, as summarized in Table 1.

Ion	Wavelength λ [Å]	Angular Resolution $\delta\theta=\lambda/D$ [mas]	Spectral Selectivity $\lambda/\Delta\lambda$	Peak Multilayer Reflectance	Effective Area A [cm^2] 2.5-m Cassegrain	2.5-m Prime-Focus
C VI	33.7	0.28	281	5.0%	122.7	2454
N VII	24.8	0.20	310	1.5%	11.0	736
O VII	22.1	0.18	295	1.0%	4.9	491
O VIII	19.0	0.16	271	0.4%	0.8	196
Fe XVII	17.0	0.14	283	0.15%	0.1	74

Table 1. Angular resolution, spectral selectivity and effective areas expected for 2.5-m Cassegrain and Prime-Focus telescopes shown in Figs. 3 and 4, at the wavelengths indicated.

3.3 A POLYCHROMATIC X-RAY INTERFEROMETER

The currently-envisioned *MAXIM* X-ray interferometry mission is directed at the development of an instrument having angular resolution of 0.01 μas or better. The primary scientific objective of this mission is to image gravitationally-broadened X-ray emission in the vicinity of the event horizon of a supermassive black hole at the center of an AGN. The baseline technical approach that has thus far emerged from the *MAXIM* study utilizes an array of grazing incidence flat mirrors, spread over a wide baseline, with each mirror located on a separate spacecraft.[13] Alternatively, a similar array of diffraction-limited normal-incidence multilayer X-ray mirrors could be used to achieve comparable performance as well.

Assuming again that 2.5-m-diameter normal-incidence multilayer mirrors are used, spread over a baseline of B=50 km, angular resolution in the range $\delta\theta=\lambda/B$=0.014 μas to 0.007 μas (over the wavelength range λ=33.7 Å – 17.0

Å) could be achieved, as summarized in Table 2. The requisite number of mirrors comprising the interferometer will ultimately be determined by the requirements on effective area and fringe reconstruction (i.e., coverage in the *u-v* plane), and these important details remain to be addressed comprehensively. Nevertheless, to take a specific example, the achievable effective areas in the case of a 32-mirror interferometer are also shown in Table 2, and range from A_{eff}=7.9 m^2 to 0.2 m^2, depending on the wavelength, again assuming currently achievable multilayer performance as described above.

In order to increase the spectral coverage of the instrument, multiple, narrow-band interferometer channels would be implemented. That is, the system would comprise separate interferometer mirror arrays, with each mirror array (of 32 mirrors, to continue with our specific example) coated with multilayers tuned to the desired wavelength. Thus to produce 3-color X-ray images, 3 separate

Figure 5. Artist's conception of an X-ray interferometer using normal-incidence multilayer X-ray mirrors.

interferometer arrays would be used (though perhaps sharing a single common detector), for a total of 3x32=96 multilayer mirrors. Greater spectral coverage would require additional mirrors. The utility of such an instrument is described in §4.2 below.
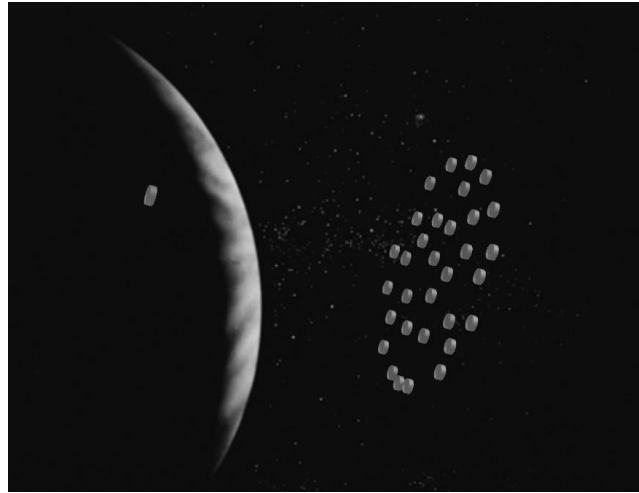
Ion	Wavelength	Angular Resolution	Spectral Selectivity	Peak Multilayer Reflectance	Effective Area
	λ [Å]	$\delta\theta=\lambda/B$ [μas]	$\lambda/\Delta\lambda$		A_{eff} [m^2]
C VI	33.7	0.014	281	5.0%	7.9
N VII	24.8	0.010	310	1.5%	2.4
O VII	22.1	0.009	295	1.0%	1.6
O VIII	19.0	0.008	271	0.4%	0.6
Fe XVII	17.0	0.007	283	0.15%	0.2

Table 2. Angular resolution, spectral selectivity and effective areas expected for an X-ray interferometer comprising an array of 32 normal-incidence multilayer mirrors, each 2.5 m in diameter, spread over a baseline of 50 km, at the wavelengths indicated.

4. OBSERVATIONAL POSSIBILITIES

4.1 SUB-MAS IMAGING USING A MONOCHROMATIC DIFFRACTION-LIMITED X-RAY TELESCOPE

Narrow-band soft X-ray imaging with angular resolution below 1 mas could be used for a variety of new observations of both Galactic and extra-Galactic sources, including stellar coronae, interacting binaries, the Galactic center, and AGN. Stars with radii R~R$_\odot$ have apparent diameters θ_D>0.1 mas at distances less than 100 pc. A monochromatic X-ray imager, tuned to one of the bright soft X-ray emission lines from such stars, having sub-mas resolution and sufficient collecting area, could be used to resolve the disks of a number of X-ray bright stars in order to address a number of questions regarding the structure and dynamics of stellar coronae, magnetic fields and flaring plasma. Outside of the Milky Way, the inner 10 pc of AGN at distances less than 200 Mpc subtend angles θ_D >10 mas; soft X-ray imaging at sub-milliarcsecond resolution could be used, therefore, to investigate the structure surrounding the

central black hole at this scale, addressing fundamental questions regarding AGN geometry and physics. Furthermore, detailed studies of the physics of relativistic AGN jets could be carried out by correlating the radio images of these structures with monochromatic X-ray images having sub-milliarcsecond resolution.

To illustrate with specific examples, we consider first Capella (α Aurigae), a well-known spectroscopic binary ($8.7R_\odot$ G8 III + $12.6R_\odot$ G1 III, P~ 104 d [14].) At a distance of d=13 pc, the two components of Capella subtend 6.2 and 9.0 mas. The *XMM-Newton* RGS spectrum[15] from Capella is shown in Fig. 6. Labeled are the bright emission lines formed in the ~10^7 K coronal gas from H- and He-like C, N and O ions, in the range $19 < \lambda < 35$ Å.

We have estimated the exposure times needed to produce images having a signal-to-noise ratio (SNR) per pixel in excess of SNR=5, assuming the Cassegrain and prime-focus telescopes described above. These results are presented in Table 3. The photon-limited SNR (i.e., ignoring any background counts) is calculated from

Figure 6. *XMM-Newton* RGS spectrum of Capella.

$$SNR^2 = \frac{A_{eff} t_{obs} f_x}{b} (\delta\theta / \theta_D)^2$$

where A_{eff} is the telescope effective area, $\delta\theta$ is the instrumental angular resolution, θ_D is the stellar diameter, and b is the image filling factor, i.e., the fraction of the stellar disk emitting at the observed wavelength.[16] The flux values f_x shown in Table 3 are computed from the measured spectrum (Fig. 6) integrated over the corresponding multilayer band-passes, which, as it happens, are especially well-matched to the observed line widths. For simplicity, we have assumed that the measured flux is distributed equally between the two stars, and have further assumed a value of b=0.1 (i.e., comparable to the Sun.)
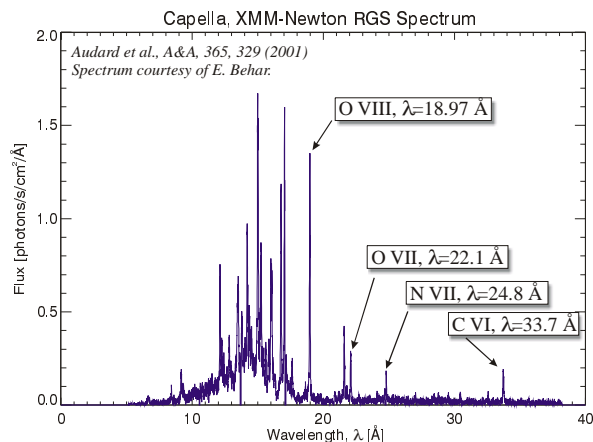
Ion	Wavelength	Capella, θ_D=6.2, 9 mas				NGC 1068, θ_D=2 as (160 pc)		
			t [s] for SNR=5				t [s] for SNR=5	
	λ [A]	f_x [ph/s/cm²]	Cassegrain		Prime-Focus	f_x [ph/s/cm²]	Cassegrain	Prime-Focus
C VI	33.7	1.82E-02	2.8E+02	2.8E+02	1.4E+01	2.9E+01	7.40E-04	1.4E+07	7.1E+05
N VII	24.8	2.56E-02	4.1E+03	4.1E+03	6.1E+01	1.3E+02	8.90E-04	2.4E+08	3.6E+06
O VII	22.1	2.48E-02	1.2E+04	1.2E+04	1.2E+02	2.5E+02	1.40E-03	4.4E+08	4.4E+06
O VIII	19.0	9.50E-02	2.6E+04	2.6E+04	1.0E+02	2.2E+02	9.80E-04	5.3E+09	2.1E+07
Fe XVII	17.0	1.10E-01	2.0E+05	2.0E+05	3.0E+02	6.3E+02	2.56E-04	1.8E+11	2.7E+08

Table 3. Exposure times required to obtain sub-mas images having SNR=5 (per pixel) of the two stars of Capella, and of the inner 2 arcseconds of the nearby AGN NGC 1068, assuming the Cassegrain and prime-focus telescopes described above in §3.

The requisite observation times listed in Table 3 are reasonably short, less than one thousand seconds, for observations made with the prime-focus instrument at all wavelengths. (We note that longer observations would of course yield higher SNRs.) The observation times are significantly larger in the case of the less efficient Cassegrain instrument, but are less than 200,000 seconds in all cases nevertheless. A number of other nearby stars having million-degree coronae, although not as bright as Capella, could be imaged similarly, albeit with somewhat longer exposure times.

Interacting binary stars offer another attractive observational target for the sub-mas X-ray telescopes considered here. The X-ray bright RS CVn binary, AR Lacertae, located at a distance of ~50 pc, has an orbital period of only 1.98 days, and a separation of only $9.22R_\odot$ (1.9 mas) between the $1.54R_\odot$ G2 IV primary and the $2.81R_\odot$ K0 IV secondary.[17]
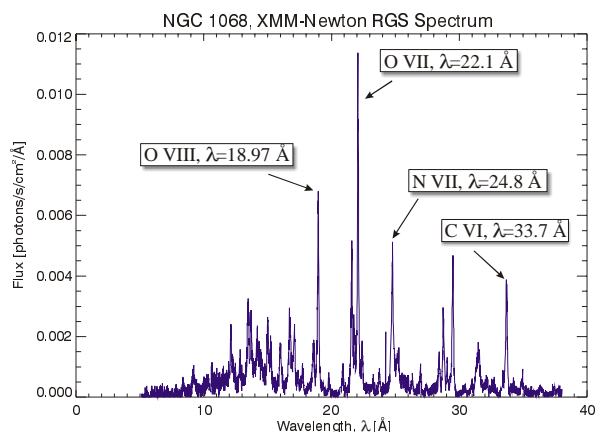
NGC 1068, XMM-Newton RGS Spectrum

Figure 7. *XMM-Newton* RGS spectrum of NGC 1068.

In this case, detailed analysis of *ASCA* data[18] suggests hot plasma exchange between the two close stars. Although the X-ray flux from this object is ~6X fainter than Capella, high-SNR, sub-mas images could be obtained in practically short observation times as well, and these images would be most revealing with regard to the spatial distribution of the X-ray emitting plasma.

As a final example we consider NGC 1068, a bright, well studied, nearby (d=16.4 Mpc[19]) Seyfert 2 galaxy. The *XMM-Newton* RGS spectrum for this object is shown in Fig. 7; again, strong emission lines from H- and He-like C, N and O ions are prominent, and arise from the radiatively-driven plasma in the circumnuclear region of this AGN.[20] The estimated observation times required to achieve SNR>5 using either a Cassegrain or prime-focus multilayer telescope are listed in Table 3. The flux values are again computed from the *XMM-Ne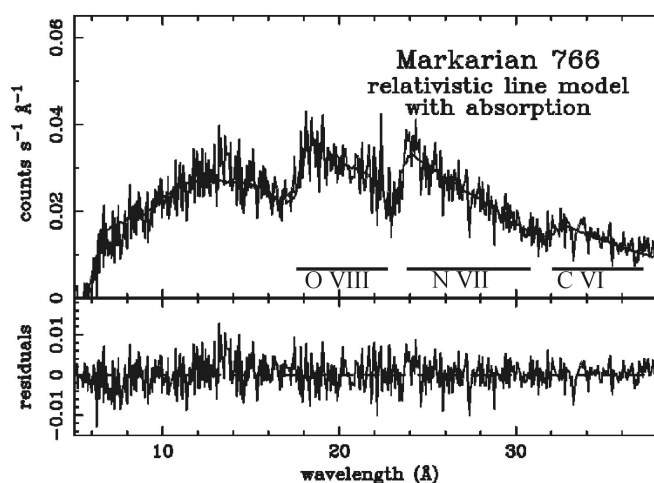wton* spectrum (Fig. 7), and we have assumed that the soft X-ray emission occurs within 2 arcseconds (160 pc) of the nucleus.[21] We have further assumed in Table 3 that observations would be re-binned with 10x degraded angular resolution. In this case high-resolution imaging is feasible (i.e., $t_{obs} < \sim 5 \times 10^6$ s) only with the prime-focus instrument, and then only for the longer wavelengths where the multilayer efficiency is greatest. (However this would certainly change with future improvements in multilayer performance.) Nevertheless, just as sub-arcsecond narrow-band optical imaging is used routinely to help elucidate the morphology of extended objects, narrow-band X-ray observations having milliarcsecond resolution of this and similar AGN would allow for correlations with milliarcsecond radio observations and high-resolution *Chandra* and *XMM-Newton* spectra.[22] Specifically, narrow-band mas X-ray images could be used to determine the precise location of the photo-ionized gas (vs. any collisionally-driven gas), and would thus address basic questions regarding the structure and dynamics of the nuclear and circumnuclear regions in AGN at sub-pc scales.[23]

4.2 SUB-μAS IMAGING USING A POLYCHROMATIC X-RAY INTERFEROMETER

A polychromatic X-ray interferometer operating in the range $16 < \lambda < 40$ Å, designed to have angular resolution of 0.01 μas or better, as sketched in §3.3, would undoubtedly lead to significant astronomical discoveries. At this resolution, observations of nearby stellar coronae and interacting binaries would result in images have detail comparable to the solar coronal images now produced by *TRACE*. Such data could be used for detailed investigations of coronal structure (including the geometry and dynamics of active regions and starspots), magnetic fields and loops, and flaring plasma.

Perhaps more significantly, angular resolution of ~0.01 μas at soft X-ray wavelengths would make possible detailed mapping of the X-ray emitting region surrounding the super-massive black holes in AGN at distances up to ~150 Mpc, the primary scientific objective of the envisioned *MAXIM* mission. As specific examples, we consider MCG—6-30-15 and Mrk 766, both narrow-line

Figure 8. XMM-Newton RGS spectrum of Mrk 766. The solid line is a fit to the data, assuming gravitationally-broadened, redshifted emission lines of O VIII, N VII, and C VI.

Seyfert 1 galaxies, with redshifts z=0.008[24] and z=0.013.[25] Assuming H_0=75 km/s/Mpc, the corresponding distances are 31 and 51 Mpc, and from the estimated central black hole masses of $2\times10^7 M_\odot$[26] and $10^7 M_\odot$[27], one gravitational radius r_g corresponds to 0.01 μas and 0.004 μas, in the case of MCG—6-30-15 and Mrk 766, respectively.

The *XMM-Newton* RGS spectra for Mrk 766 is shown in Fig. 8;[28] the spectrum for MCG—6-30-15, although not shown here, is similar. The broad features from ~18 – 35 Å have been identified as relativistically broadened Ly-α emission lines of O VIII, N VII and C VI, as indicated in the figure, produced in the inner-most region of an accretion disk around a Kerr black hole. Assuming that this interpretation is correct, two or more discrete multilayer channels of a soft X-ray interferometer could be used to produce a high resolution velocity map of this region.

With an effective area of 2.4 m^2 per channel (each over a 0.08 Å bandpass) centered on the broadened N VII line (i.e., in the range λ=24 – 28 Å), for example, we estimate from the spectrum shown in Fig. 8 a count rate of ~1.2 photons/s for Mrk 766 (and approximately the same count rate for MCG—6-30-15.) With 32 mirrors comprising each interferometer channel (i.e., 16 effective fringe sets), assuming that fringe modulation of 50% could be achieved, we estimate that a high resolution image could be obtained in t_{obs}~8×10^5 s for either MCG—6-30-15 or Mrk 766 (assuming that $\lambda/\Delta\lambda$~300 fringes are observed, and that 50 photons/fringe are required.[29]) Such results would elucidate the structure and dynamics of the accretion disk to within ~2.5 r_g of the black hole for Mrk 766, and within ~1 r_g in the case of MCG—6-30-15, whereas much of the relativistically broadened X-ray emission is thought to occur within $6 – 20 r_g$.[30] More massive and/or closer AGN would afford detailed mapping at even smaller radii. We emphasize again that future improvements in multilayer technology would result in greater SNR and/or reduced observation times.

5. SUMMARY

We have described the current state-of-the-art of commercially available, normal-incidence mirror substrates that are diffraction limited to ~$\lambda_{34Å}$ /10, or ~$\lambda_{17Å}$ /5, and recently developed ultra-short-period X-ray multilayer coatings that operate near normal incidence at wavelengths as small as λ=16 Å. These technologies could be used to construct diffraction-limited X-ray telescopes having sub-mas resolution and large effective area at judiciously chosen soft X-ray wavelengths (i.e., corresponding to bright emission lines of, e.g., C VI, N VII, O VII, O VIII and Fe XVII produced in many astrophysical plasmas). We have outlined how such telescopes would enable high-resolution, narrow-band ($\lambda/\Delta\lambda$~300) imaging, in essence a new observational technique for X-ray astronomy, analogous to the narrow-band imaging now performed routinely in other parts of the spectrum using filters. This observational approach would complement more traditional X-ray techniques (i.e., broad-band imaging and high-resolution spectroscopy) for a variety of objects. We have also sketched how this technology could ultimately be used to construct a soft X-ray interferometer, for polychromatic imaging with angular resolution of $\delta\theta$~0.01 μas or better, in order to produce velocity maps from the gravitationally-broadened X-ray emission due to hot material near the event horizon of a super-massive black hole, the primary scientific objective of the *MAXIM* mission.

There are clearly a number of major technical and economic challenges that must be addressed in order to realize the full potential for astronomy of the normal-incidence X-ray mirror technology we have described here. We have not discussed here even the most basic engineering challenges, such as the stringent performance requirements on alignment, pointing, target acquisition and station-keeping that must be met. Nevertheless, these challenges are essentially common to all technical approaches towards sub-mas X-ray imaging and sub-μas X-ray interferometry. Our hope is simply that research will be carried out on the normal-incidence mirror technology described here, as well as on other viable technologies, in order that the most optimal technical approach can eventually be identified and pursued.

ACKNOWLEDGEMENTS

REFERENCES

[1] J.P. Delaboudinière, *et al*. *Solar Physics* 162, 291 (1995)

[2] T.D. Tarbell, *et al*., Proc. 3rd SoHO Workshop, ESA SP-373 (1994)

[3] B.N. Handy, *et al*., *Solar Physics*, 187, 229 (1999)

[4] see, for example, K. C. Gendreau, *et al*, these proceedings (#4851-39)

[5] D.A. Tichenor, *et al*., Proc. SPIE 4343, 19 (2001)

[6] G. E. Sommargren, *OSA Trends in Optics and Photonics Vol. 4, Extreme Ultraviolet Lithography*, Kubiak and Kania, eds. (Optical Society of America, Washington, DC 1996), pp. 108-112

[7] H. Medecki, E. Tejnil, K. A. Goldberg, and J. Bokor, *Opt. Lett*., 21, 1526 (1996)

[8] D. L. Windt and W. K. Waskiewicz, *J. Vac. Sci. Technol. B*, 12, 3826 (1994)

[9] R. Soufli, *et al*., *Proc. SPIE*, 4343, 51, (2001)

[10] F. Schäfers, *et al*., *Nucl. Instr. Meth. A*, 467-468, 349 (2001)

[11] F. Eriksson, G. A. Johansson, H. M. Hertz, and J. Birch, *Proc. SPIE*, 4506, 14 (2001)

[12] D. L. Windt, E. M. Gullikson, C. C. Walton, *Opt. Lett., in press* (2002)

[13] W. Cash, A. Shipley, S. Osterman, M. Joy, *Nature*, 407, 160 (2000)

[14] C. A. Hummel, *et al*., *AJ*, 107, 1859 (1994)

[15] M. Audard, M. Güdel, R. Mewe, *A&A*, 365, L318 (2001)

[16] J. Linsky, presented at the *MAXIM* meeting, Boulder, CO, January 1999.

[17] C. R. Chambliss, *PASP*, 88, 762 (1976)

[18] M. Siarkowski, *et al*., *ApJ*, 473, 470 (1996)

[19] F.C. Bruhweiler, *et al*., *ApJ*, 546, 866 (2001)

[20] A. Kinkhabwala, *et al*., astro/ph-0107224 (2002)

[21] A. S. Wilson, *et al*., *ApJ*, 391, L75 (1992)

[22] A.J. Young, A.S. Wilson, and P. L.Shopbell, *ApJ*, 556, 6 (2001)

[23] M. Elvis, *ApJ*, 545, 63 (2000)

[24] K. B. Fisher, J. P. Huchra, M. A. Strauss, *et al*. 1995, ApJS, 100, 69

[25] B. J. Smith, S. G. Kleinmann, J. P. Huchra, & F. J. Low, *ApJ*, 318, 161 (1987)

[26] C. S. Reynolds, *ApJ*, 533, 811 (2000)

[27] A. Laor, *ApJ*, 553, 677 (2001)

[28] G. Branduari-Raymont, *et al*, *A&A*, 365, L140 (2001); M. Sako, *et al*., astro/ph-0112436 (2001)

[29] M. Elvis, presented at the *MAXIM* meeting, Boulder, CO, January 1999.

[30] Y. Dabrowski, *et al*., *MNRAS*, 288, L11 (1997)